

The BMV project: Search for photon oscillations into massive particles

C. Robilliard, B. Pinto Da Souza, F. Bielsa, J. Mauchain, M. Nardone, G. Bailly, M. Fouché, R. Battesti, and C. Rizzo

Abstract: In this contribution to PSAS08 we report on the research activities developed in our Toulouse group, in the framework of the BMV project, concerning the search for photon oscillations into massive particles, such as axion-like particles in the presence of a strong transverse magnetic field. We recall our main result obtained in collaboration with LULI at École Polytechnique (Palaiseau, France). We also present the very preliminary results obtained with the BMV experiment which is set up at LNCMP (Toulouse, France).

Résumé : Dans cette contribution à PSAS08, nous présentons les activités de recherche développées dans notre groupe à Toulouse, dans le cadre du projet BMV, concernant la recherche d'oscillations entre photons et particules massives telles que les pseudo-axions en présence d'un champ magnétique transverse intense. Nous rappelons notre principal résultat obtenu en collaboration avec le LULI à l'École Polytechnique (Palaiseau, France). Nous présentons également les résultats très préliminaires obtenus sur l'expérience BMV, installée au LNCMP (Toulouse, France).

In Toulouse (France), since 2001 we have been conducting research activities in the framework of the BMV (Biréfringence Magnétique du Vide) project [1] to study the propagation of light in the presence of intense transverse magnetic fields, with the goal to observe for the first time the vacuum magnetic birefringence. This is a very fundamental prediction of quantum electrodynamics that has never been experimentally proved (see [2] and references therein).

In 1986, Maiani, Petronzio, and Zavattini [3] showed that a hypothetical low mass, neutral, spinless boson, scalar or pseudoscalar, that couples with two photons could induce an ellipticity signal in the apparatus designed to measure QED vacuum magnetic birefringence [4]. Moreover, an apparent rotation of the polarization vector of light could be observed because of the conversion of photons into real bosons, resulting in a vacuum magnetic dichroism which is absent in the framework of standard QED. The measurements of ellipticity and dichroism, including their signs, can in principle completely characterize the hypothetical boson, its mass m_a , the inverse coupling constant M , and the pseudoscalar or scalar nature of the particle. Ellipticity and dichroism are two different facets of the same phenomenon: oscillation of photons into massive virtual or real particles. Maiani, Petronzio, Zavattini's paper was essentially motivated by the search for Peccei and Quinn's axion [5].

The axion is a particle beyond the Standard Model. Proposed more than 30 years ago to solve

Received . Revision received . Accepted . Revision accepted .

C. Robilliard,¹ B. Pinto Da Souza, G. Bailly, M. Fouché, and C. Rizzo. Laboratoire Collisions Agrégats Réactivité, IRSAMC, UPS/CNRS, UMR 5589, 31062 Toulouse, France.

F. Bielsa, J. Mauchain, M. Nardone, and R. Battesti. Laboratoire National des Champs Magnétiques Pulsés, CNRS/INSA/UPS, UMR 5147, 31400 Toulouse, France.

¹Corresponding author (e-mail: email: cecile.robilliard@irsamc.ups-tlse.fr).

the strong CP problem [5, 6], this neutral, spinless, pseudoscalar particle has not been detected yet, in spite of constant experimental efforts [7–10]. Whereas the most sensitive experiments aim at detecting axions of solar or cosmic origin, laboratory experiments including the axion source do not depend on models of the incoming axion flux. Because the axion is not coupled to a single photon but to a two-photon vertex, axion-photon conversion requires an external electric or - preferentially - magnetic field to provide for a virtual second photon [11].

At present, purely terrestrial experiments are built according to two main schemes. The first one, following the 1979 Iacopini and Zavattini proposal [4], is sensitive to the ellipticity and, slightly modified, to the dichroism induced by the coupling of low mass, neutral, spinless bosons with laser beam photons and the magnetic field [3]. The second popular experimental scheme, named “light shining through the wall” [12], consists of first converting incoming photons into axions in a transverse magnetic field, then blocking the remaining photon beam with an opaque wall. Behind this wall with which the axions do not interact, a second magnetic field region allows the axions to convert back into photons with the same frequency as the incoming ones. Counting these regenerated photons, one can calculate the axion-photon coupling or put some limits on it. This set-up was first realized by the BFRT collaboration in 1993 [7].

Due to their impressive precision, optical experiments relying on couplings between photons and these hidden-sector particles seem most promising. Thanks to such couplings, the initial photons oscillate into the massive particle to be detected. The strength of optical experiments lies in the huge accessible dynamical range: from more than 10^{20} incoming photons, one can be sensitive to 1 regenerated photon!

In fact, the “light shining through the wall” experiment also yields some valuable information on another hidden-sector hypothetical particle [13]. After the observation of a deviation from blackbody curve in the cosmic background radiation [14], some theoretical works suggested photon oscillations into a low mass hidden sector particle as a possible explanation [15]. The supporting model for such a phenomenon is a modified version of electrodynamics proposed in 1982 [16], based on the existence of two U(1) gauge bosons. One of the two can be taken as the usual massless photon, while the second one corresponds to an additional massive particle usually called paraphoton. Both gauge bosons are coupled, giving rise to photon-paraphoton oscillations. Several years later, more precise observations did not confirm any anomaly in the cosmic background radiation spectrum [17] and the interest for paraphoton decreased, although its existence was not excluded. More recently, it was found out that similar additional U(1) gauges generally appear in string embeddings of the standard model [18], reviving the interest for experimental limits on the paraphoton parameters [19–21]. Some limits on the mass and the coupling constant of the paraphoton have already been obtained by a photoregeneration experiment [7].

Motivated by the observation published by the PVLAS collaboration, and subsequently retracted [22], which they claimed could be explained by the existence of axions in the mass range 1-2 meV, we have performed a “light shining through the wall” experiment in collaboration with LULI at École Polytechnique (Palaiseau, France). We proved that the PVLAS signal was not due to the existence of axions [23]. We recall here our main results [24]. We also present the very preliminary results obtained with the BMV experiment which is set up at LNCMP (Toulouse, France) [2]. From the technological point of view, both experiments rely on pulsed magnets to deliver the high transverse magnetic fields needed. The coils we used have been especially designed and developed in the framework of our project [25].

1. “Light shining through the wall” experiment at LULI

This experiment has been described in details in ref. [24]. We recall here the main points.

1.1. Axion-like particles

The photon to axion-like particle conversion and reconversion transition probability (in natural units $\hbar = c = 1$, with $1 \text{ T} \equiv 195 \text{ eV}^2$ and $1 \text{ m} \equiv 5 \times 10^6 \text{ eV}^{-1}$) after propagating over a distance L in a homogeneous magnetic field B_0 writes

$$p_a = (\Delta_M L)^2 \frac{\sin^2\left(\frac{\Delta_{\text{osc}} L}{2}\right)}{\left(\frac{\Delta_{\text{osc}} L}{2}\right)^2}, \quad (1)$$

where $\Delta_M = \frac{B_0}{2M}$ and $\Delta_{\text{osc}} = \frac{m_a^2}{2\omega}$, ω being the photon energy, m_a the axion-like particle mass and M its inverse coupling constant with two photons. In our case, our search was focused on the mass range $1 \text{ meV} < m_a < 2 \text{ meV}$. Note that this equation is valid for a light polarization parallel to the magnetic field since the axion has to be a pseudoscalar [5]. Finally, for two identical magnets, the photon regeneration probability due to axion-like particles is $P_a = p_a^2$.

1.2. Paraphotons

As far as paraphoton is concerned, in the modified version of electrodynamics developed in 1982 [16], the paraphoton weakly couples with the photon through kinetic mixing. Contrary to axion-like particles, photon-paraphoton oscillations are therefore possible without any external field and are independent on photon polarization.

In the case of a typical photoregeneration experiment, the incoming photons freely propagate for a distance L_1 and might oscillate into paraphotons before being stopped by a wall, after which the paraphotons propagate for a distance L_2 and have a chance to oscillate back into photons that are detected. The photon regeneration probability due to paraphotons can therefore be written as:

$$\begin{aligned} P_\gamma &= p_\gamma(L_1)p_\gamma(L_2) \\ &= 16\chi^4 \sin^2\left(\frac{\mu^2 L_1}{4\omega}\right) \sin^2\left(\frac{\mu^2 L_2}{4\omega}\right) \end{aligned} \quad (2)$$

where χ is the photon-paraphoton coupling constant, and μ is the paraphoton mass which arbitrary values are to be determined experimentally.

In our experiment, L_1 is the distance between the focusing lens at the entrance of the vacuum system, which focuses photons but not paraphotons, and the wall, which blocks photons only. Similarly, L_2 represents the distance separating the blind flange just before the regenerating magnet and the lens coupling the regenerated photons into the optical fibre (see Fig. 1).

1.3. Experimental set-up

As shown in Fig. 1, the experimental setup consists of two main parts separated by the wall. An intense laser beam travels through a first magnetic region (generation magnet) where photons might be converted into axion-like particles. The wall blocks every incident photons while axion-like particles would cross it without interacting and may be converted back into photons in a second magnetic region (regeneration magnet). The regenerated photons are finally detected by a single photon detector.

The three key elements leading to a high detection rate are the laser, the generation and regeneration magnets placed on each side of the wall and the single photon detector.

In order to have the maximum number of incident photons at a wavelength that can be efficiently detected, the experiment has been set up at Laboratoire pour l'Utilisation des Lasers Intenses (LULI) in Palaiseau, on the Nano 2000 chain [26]. It can deliver more than 1.5 kJ over a few nanoseconds with $\omega = 1.17 \text{ eV}$. This corresponds to $N_i = 8 \times 10^{21}$ photons per pulse. During our 4 weeks of campaign,

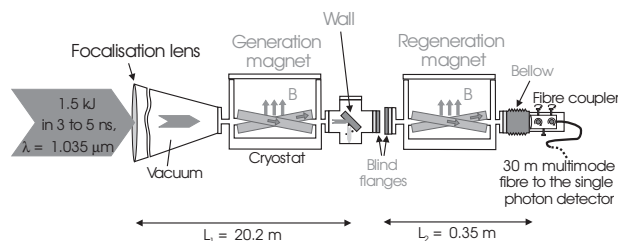


Fig. 1. Sketch of the apparatus. The wall and the blind flanges are removable for fibre alignment.

the total pulse duration ranged from 5 ns to 3 ns while keeping the total energy constant. At the end of the amplification chain, the vertically linearly polarized incident beam has a 186 mm diameter and is almost perfectly collimated. It is then focused using a lens which focal length is 20.4 m. The wall is placed at $L_1 = 20.2$ m from the lens in order to have the focusing point a few centimeters behind this wall. The beam is well apodized to prevent the incoming light from generating a disturbing plasma on the sides of the vacuum tubes.

In the region before the wall, where the laser beam propagates, a vacuum better than 10^{-3} mbar is necessary in order to avoid air ionization. Two turbo pumps along the vacuum line easily give 10^{-3} mbar near the lens and better than 10^{-4} mbar close to the wall. The wall is made of a 15 mm width aluminum plate to stop every incident photon. It is tilted by 45° with respect to the laser beam axis in order to increase the area of the laser impact and to avoid retroreflected photons. In the second magnetic field region, a vacuum better than 10^{-3} mbar is also maintained.

Concerning the magnets, we use a pulsed technology. The pulsed magnetic field is produced by a transportable generator developed at LNCMP [27], which consists of a capacitor bank releasing its energy in the coils in a few milliseconds. Besides, a special coil geometry has been developed in order to reach the highest and longest transverse magnetic field. The coil properties are explained in details in Ref. [25]. A coil consists of two interlaced race-track shaped windings that are tilted one with respect to the other. This makes room for the necessary optical access at both ends in order to let the laser in while providing a maximum $B_0 L$. Because of the particular arrangement of wires, these magnets are called Xcoils. The coil frame is made of G10 which is a non conducting material commonly used in high stress and cryogenic temperature conditions. External reinforcements with the same material have been added after wiring to contain the magnetic pressure that can be as high as 500 MPa. A 12 mm diameter aperture has been dug into the magnets for the light path. As for usual pulsed magnets, the coils are immersed in a liquid nitrogen cryostat to limit the consequences of heating. The whole cryostat is double-walled for a vacuum thermal insulation. This vacuum is common with the vacuum line and is better than 10^{-4} mbar. A delay between two pulses is necessary for the magnet to cool down to the equilibrium temperature which is monitored via the Xcoils' resistance. Therefore, the repetition rate is set to 5 pulses per hour. The magnetic field is measured by a calibrated pick-up coil. The maximum field B_0 is obtained at the center of the magnet. Xcoils have provided $B_0 \geq 13.5$ T over an equivalent length $L = 365$ mm. However, during the whole campaign a lower magnetic field of $B_0 = 12$ (0.3) T was used to increase the coils' lifetime. The total duration of a magnetic pulse is a few milliseconds. The magnetic field reaches its maximum value within less than 2 ms and remains constant ($\pm 0.3\%$) during $\tau_B = 150 \mu\text{s}$, a very long time compared to the laser pulse.

The last key element is the detector that has to meet several criteria. In order to have as good a sensitivity as possible, the regenerated photon detection has to be at the single photon level. The integration time is limited by the longest duration of the laser pulse which is 5 ns. Since we expected about 100 laser pulses during our four week campaign, which corresponds to a total integration time of 500 ns,

we required a detector with a dark count rate far lower than 1 over this integration time, so that any increment of the counting would be unambiguously associated to the detection of one regenerated photon. Our detector is a commercially available single photon receiver from Princeton Lightwave which has a high detection efficiency at $1.05 \mu\text{m}$. It integrates a $80 \times 80 \mu\text{m}^2$ InGaAs Avalanche Photodiode (APD) with all the necessary bias, control and counting electronics. Light is coupled to the photodiode through a FC/PC connector and a multimode fiber. When the detector is triggered, the APD bias voltage is raised above its reverse breakdown voltage V_{br} to operate in “Geiger mode”. A short time later – adjustable between 1 ns and 5 ns – the bias is reduced below V_{br} to avoid false events. For our experiment, the bias pulse width is 5 ns to correspond with the longest laser pulse. To optimize the dark count rate and the detection efficiency η_{det} , three different parameters can be adjusted: the APD temperature, the discriminator threshold V_{d} set to reject electronic noise and the APD bias voltage V_{APD} . The dark count rate is first minimized by choosing the lowest achievable temperature which is around 221 K. Dark counts for a 5 ns detection gate as a function of V_{d} increase rapidly when V_{d} is too low. On the other hand, η_{det} remains constant for a large range of V_{d} . We set V_{d} to a value far from the region where dark count increases and where η_{det} is still constant. This corresponds to less than 2.5×10^{-2} dark count over 500 ns integration time. The detection efficiency is precisely measured by illuminating the detector with a laser intensity lower than 0.1 photon per detection gate at $1.05 \mu\text{m}$. The probability to have more than one photon per gate is thus negligible. The best compromise between detection efficiency and dark count rate is found for $\eta_{\text{det}} = 0.48(0.025)$.

As said in the introduction, other similar experiments generally require long integration times which implies an experimental limitation due to the detection noise. Using pulsed laser, magnetic field and detection is an original and efficient way to overcome this problem. Photons are concentrated in very intense short laser pulses during which the detection background is negligible. This also means that if a photon is detected in our experiment in correlation with the magnetic field, it will be an unambiguous signature of axion generation inside our apparatus.

After the second magnet, the regenerated photons are injected into the detector through a coupling lens and a graded index multimode fiber with a $62.5 \mu\text{m}$ core diameter, a 0.27 numerical aperture and an attenuation lower than 1 dB/km. These parameters ensure that we can inject light into the fiber with a high coupling ratio, even when one takes into account the pulse by pulse instability of the propagation axis that can be up to $9 \mu\text{rad}$. During data acquisition, the mean coupling efficiency through the fibre was found to be $\eta_c = 0.85$; it was optimized just before each pulse with an attenuated beam originating from the same pilot, hence exactly superimposed to the high energy beam used for the measurements. The only remaining source of misalignment lies in thermal effects during the high energy pulse, which could slightly deviate the laser beam, hence generating supplementary losses in fibre coupling. This misalignment is mostly reproducible and can be corrected by acting on the mirrors steering the beam to the wall.

Our experiment is based on pulsed elements which require a perfect synchronization : the laser pulse must cross the magnets when the magnetic field is maximum and fall on the photodiode during the detection gate. The magnetic pulse is triggered with a TTL signal from the laser chain. The magnetic trigger has a jitter lower than $10 \mu\text{s}$, ensuring that the laser pulse travels through the magnets within the $150 \mu\text{s}$ interval during which the magnetic field is constant and maximum. Synchronization of the laser pulse and the detector needs to be far more accurate since both have a 5 ns duration. The detector gate is triggered with the same fast signal as the laser, using delay lines. We have measured the coincidence rate between the arrival of photons from the attenuated beam described above on the detector and the opening of the 5 ns detector gate as a function of an adjustable delay [24]. We have chosen our working point in order to maximize the coincidence rate.

1.4. Data analysis

The best experimental limits are achieved if no fake signal is detected during the experiment, which was indeed the case. To estimate the corresponding upper conversion probability of regenerated photons, we have to calculate the upper number of photons that could have been missed by the detector n_{missed} for a given confidence level (CL), which writes

$$n_{\text{missed}} = \frac{\log(1 - CL)}{\log(1 - \eta_{\text{det}})} - 1. \quad (3)$$

For example, with our value of η_{det} , a confidence level of 99.7% corresponds to less than 8 missed photons. The upper photon regeneration probability is then

$$P_{\text{a or } \gamma} = \frac{n_{\text{missed}}}{N_{\text{eff}}}, \quad (4)$$

where N_{eff} is the number of effective incident photons over the total number of laser shots, taking into account the losses described before.

Data acquisition was spread over 4 different weeks. 82 high energy pulses have reached the wall with a total energy of about 110 kJ. This corresponds to 5.9×10^{23} photons. During the whole data acquisition, no signal has been detected. The magnetic field was applied during 56 of those laser pulses, with a mean value of 12 T. The laser pulses without magnetic field aimed at testing for possible fake counts.

Our experimental sensitivity limits for axion-like particle at 99.7% confidence level correspond to a detection probability of regenerated photons $P_{\text{a}} = 3.3 \times 10^{-23}$ and give $M > 9.1 \times 10^5$ GeV at low masses [24]. We show our limits together with those from other laboratory experiments in Fig. 2. They are comparable to the limits obtained by other purely laboratory experiments [7, 28, 29], especially in the meV region of mass. On the other hand, they are still much less sensitive than experiments which limits (stripes) approach model predictions [8, 9, 30, 31].

In the case of paraphotons our measurements correspond to a maximum photon regeneration probability $P_{\gamma} = 9.4 \times 10^{-24}$. This sets a limit $\chi < 1.1 \times 10^{-6}$ for $1 \text{ meV} < \mu < 10 \text{ meV}$ with a 95% confidence level. As shown in Fig. 3, this improves by about one order of magnitude the exclusion area obtained on BFRT photon regeneration experiment [7]. Comparing to other laboratory experiments [34, 35] (see [36] for review), we were able to constrain the paraphoton parameters in a region which had not been covered so far by purely terrestrial experiments.

2. The BMV experiment at LNCMP

This experiment has been described in details in ref. [2]. We recall here the main points and present our very preliminary results.

Linearly polarized light, propagating in a medium in the presence of a transverse magnetic field, acquires an ellipticity [37]. Indeed, the velocity of light propagating in the presence of a transverse magnetic field B depends on the light polarization, i.e. the index of refraction n_{\parallel} for light polarized parallel to the magnetic field is different from the index of refraction n_{\perp} for light polarized perpendicular to the magnetic field. For symmetry reasons, the difference $\Delta n = (n_{\parallel} - n_{\perp})$ is proportional to B^2 . Thus, in general an incident linearly polarized light beam exits elliptically polarized from the magnetic field region. Quantum ElectroDynamics (QED) predicts that a field of 1 T should induce an anisotropy of the index of refraction of vacuum Δn of about 4×10^{-24} [38, 39].

Photon oscillations into a virtual massive particle like axions also induce an ellipticity signal ψ in such an apparatus [3]. This ellipticity can be written as [7] :

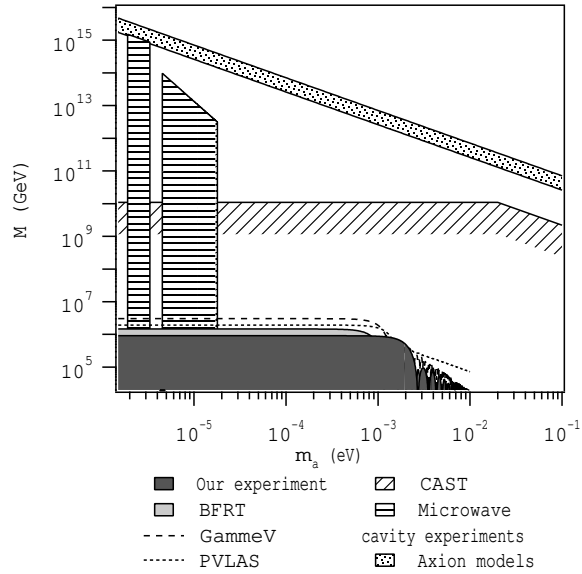


Fig. 2. Limits on the axion-like particle - two photon inverse coupling constant M as a function of the axion-like particle mass m_a obtained by experimental searches. Our exclusion region is first compared to other purely laboratory experiments such as the BFRT photon regeneration experiment [7], the GammeV experiment [28] and the PVLAS collaboration [29] with a 3σ confidence level. Those curves are finally compared to the 95 % confidence level exclusion region obtained on CAST [9] and the more than 90 % confidence level on microwave cavity experiments [8, 30, 31]. Model predictions are also shown as a dotted stripe between the predictions of the KSVZ model (lower line, $E/N = 0$) [32] and of the DFSZ model (upper line, $E/N = 8/3$) [33].

$$\psi = \left(\frac{\Delta_M^2 L}{\Delta_{\text{osc}}} \right) \left(1 - \frac{\sin(\Delta_{\text{osc}})}{\Delta_{\text{osc}}} \right), \quad (5)$$

where $\Delta_M = \frac{B_0}{2M}$ and $\Delta_{\text{osc}} = \frac{m_a^2}{2\omega}$, ω being the photon energy, m_a the axion-like particle mass and M its inverse coupling constant with two photons. Moreover, since we use an optical resonant cavity to increase the optical path in the magnetic field region, the ellipticity acquired by the light is increased by a factor $\frac{2F}{\pi}$, where F is the finesse of the optical cavity. The finesse is related to the photon lifetime τ in the cavity by the formula $\tau = \frac{FL}{\pi c}$, where c is the light velocity.

During our first run once the whole apparatus was operational, we have measured the magnetic birefringence of molecular Nitrogen. Our experimental value $\Delta n = (-2.49 \pm 0.05) \times 10^{-13}$ at 1 atm and 273.15 K is in good agreement with other existing values [37]. We have also acquired data in vacuum to search for vacuum magnetic birefringence. After 17 magnetic field pulses with $B_0 \simeq 9$ T over a length about 0.5 m and a cavity finesse $F \simeq 3000$, we have reached a value Δn per T^2 of $(-10 \pm 23) \times 10^{-17} \text{ T}^{-2}$, which is obviously compatible with zero. In Fig. 4 we show the limit obtained on the parameters of axion-like particles by this ellipticity measurement, together with the one obtained by our group at LULI.

Recently we have upgraded our optical cavity to reach a higher finesse and thus a better sensitivity. In Fig. 5 we show a photon lifetime measurement, corresponding to $\tau \simeq 190 \mu\text{s}$ and $F \simeq 80000$ [40]. Such a photon lifetime in a cavity is one of the longest ever measured (see e.g. [41]).

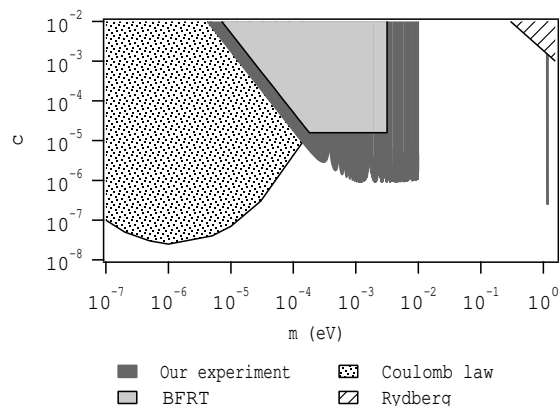


Fig. 3. 95 % confidence level limits on photon-paraphoton mixing parameter as a function of the paraphoton mass obtained thanks to our null result (deep gray area). Shaded regions are excluded. This is compared to excluded regions obtained on BFRT photon regeneration experiment [7] (light gray area), to searches for deviations of the Coulomb law [34] (points) and to comparisons of the Rydberg constant for different atomic transitions [35] (stripes).

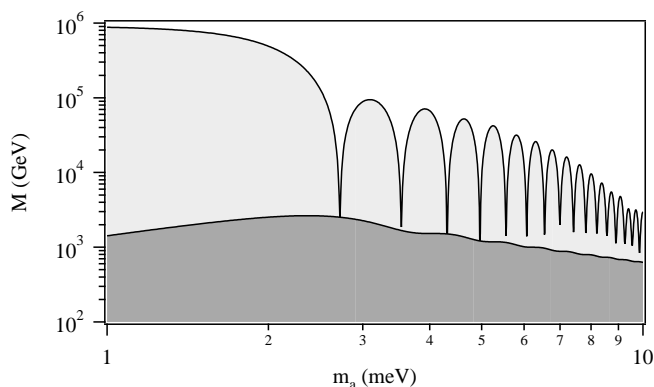


Fig. 4. Excluded mass m_a and inverse coupling constant M for axion-like particles, obtained respectively by the measurement of a zero ellipticity on the BMV experiment (dark grey) and the null result of our photoregeneration experiment at LULI (light grey).

3. Conclusion and Outlooks

We have presented the final results of our photon regeneration experiment which excluded the PVLAS results. Our null measurement leads to limits similar to other purely terrestrial axion searches, and improves the preceding limits by more than one order of magnitude concerning paraphotons [19].

Some further improvements on axion-like particles are to be expected from our BMV experiment, which is now operational. A first run has been performed. The limit obtained by ellipticity measurements is still far from being innovative but it is nevertheless encouraging, and the final set-up should allow us to improve by one to two orders of magnitude the present best limit on axion-like particles from purely terrestrial experiments.

More generally, let us argue that such precision optical experiments may prove useful for experi-

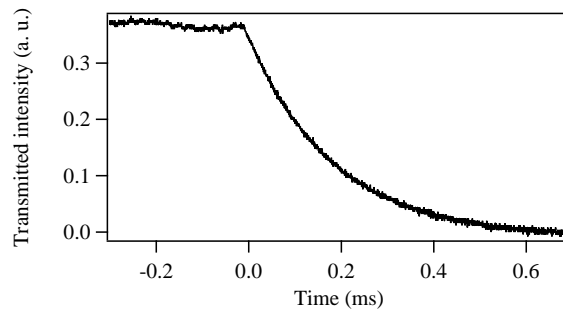


Fig. 5. Typical measurement of photon lifetime in the optical cavity, corresponding to $\tau \simeq 190 \mu\text{s}$ and $F \simeq 80000$.

mentally testing the numerous theories beyond standard model in the low energy window, a range in which the large particle accelerators are totally helpless. For example, our apparatus can be modified to become sensitive to chameleon fields [42].

References

1. S. Askenazy, *et al.*, *AIP Conf. Proc.* **564**, 115 (2001).
2. R. Battesti, *et al.*, *Eur. Phys. J. D* **46**, 323 (2008).
3. L. Maiani, R. Petronzio and E. Zavattini, *Phys. Lett. B* **175**, 359 (1986).
4. E. Iacopini and E. Zavattini, *Phys. Lett. B* **85**, 151 (1979).
5. R. D. Peccei and H. R. Quinn, *Phys. Rev. Lett.* **38**, 1440 (1977); R. D. Peccei and H. R. Quinn, *Phys. Rev. D* **16**, 1791 (1977).
6. S. Weinberg, *Phys. Rev. Lett.* **40**, 223 (1978); F. Wilczek, *Phys. Rev. Lett.* **40**, 279 (1978).
7. R. Cameron *et al.*, *Phys. Rev. D* **47**, 3707 (1993).
8. S. J. Asztalos, *et al.*, *Phys. Rev. D* **69**, 011101(R) (2004); L.D. Duffy *et al.*, *Phys. Rev. D* **74**, 012006 (2006).
9. S. Andriamonje *et al.* (CAST collaboration), *J. Cosmol. Astropart. Phys.* **04**, 010 (2007).
10. For a review, see G. G. Raffelt, *J. Phys. A* **40**, 6607 (2007) and references therein.
11. P. Sikivie, *Phys. Rev. Lett.* **51**, 1415 (1983); P. Sikivie, *Phys. Rev. D* **32**, 2988 (1985).
12. K. Van Bibber *et al.*, *Phys. Rev. Lett.* **59**, 759 (1987).
13. V.V. Popov and O.V. Vasil'ev, *Europhys. Lett.* **15**, 7 (1991).
14. D.P. Woody and P.L. Richards, *Phys. Rev. Lett.* **42**, 925 (1979).
15. H. Georgi, P. Ginsparg and S.L. Glashow, *Nature* **306**, 765 (1983); M. Axenides and R. Brandenberger, *Phys. Lett. B* **134**, 405 (1984).
16. L. B. Okun, *Zh. Eksp. Teor. Fiz.* **83**, 892 (1982) [*Sov. Phys. JETP* **56**, 502 (1982)].
17. J.C. Mather *et al.*, *Astrophys. J. Lett.* **354**, L37 (1990); H.P. Gush, M. Halpern and E.H. Wishnow, *Phys. Rev. Lett.* **65**, 537 (1990).
18. S. Abel and J. Santiago, *J. Phys. G* **30**, R83 (2004); R. Blumenhagen *et al.*, *Phys. Rep.* **445**, 1 (2007).
19. M. Ahlers *et al.*, *Phys. Rev. D* **76**, 115005 (2007).
20. J. Jaeckel and A. Ringwald, *Phys. Lett. B* **659**, 509 (2008).
21. M. Ahlers *et al.*, *Phys. Rev. D* **77**, 095001 (2008).
22. E. Zavattini *et al.*, *Phys. Rev. Lett.* **96**, 110406 (2006); *ibid.* **99**, 129901 (2007).
23. C. Robilliard *et al.*, *Phys. Rev. Lett.* **99**, 190403 (2007).
24. M. Fouché *et al.*, *Phys. Rev. D* **78**, 032013 (2008).
25. S. Batut *et al.*, *IEEE Trans. Applied Superconductivity*, **18**, 600 (2008).
26. See <http://www.luli.polytechnique.fr/pages/LULI2000.htm>
27. P. Frings *et al.*, *Rev. of Sc. Inst.* **77**, 063903 (2006).

28. A. S. Chou *et al.*, Phys. Rev. Lett. **100**, 080402 (2008).
29. E. Zavattini *et al.*, Phys. Rev. D **77**, 032006 (2008).
30. S. DePanfilis *et al.*, Phys. Rev. Lett. **59**, 839 (1987); W. U. Wuensch *et al.*, Phys. Rev. D **40**, 3153 (1989).
31. C. Hagmann *et al.*, Phys. Rev. D **42**, 1297 (1990).
32. J. E. Kim, Phys. Rev. Lett. **43**, 103 (1979); M.A. Shifman, A.I. Vainshtein and V.I. Zakharov, Nucl. Phys. B **166**, 493 (1980).
33. M. Dine, W. Fischler and M. Srednicki, Phys. Lett. B **104**, 199 (1981); A.P. Zhitnitskii, Sov. J. Nucl. Phys. **31**, 260 (1980).
34. G. D. Cochran and P. A. Franken, Bull. Am. Phys. Soc. **13**, 1379 (1968); D. F. Bartlett, P. E. Goldhagen and E. A. Phillips, Phys. Rev. D **2**, 483 (1970); E. R. Williams, J. E. Faller and H. A Hill, Phys. Rev. Lett. **26**, 721 (1971).
35. R. G. Beausoleil *et al.*, Phys. Rev. A **35**, 4878 (1987).
36. D. F. Bartlett and S. Logl, Phys. Rev. Lett. **61**, 2285 (1988).
37. C. Rizzo, A. Rizzo and D. M. Bishop, Int. Rev. Phys. Chem. **16**, 81 (1997).
38. Z. Bialynicka-Birula and I. Bialynicki-Birula, Phys. Rev. D **2**, 2341 (1970).
39. S. L. Adler, Ann. Phys. (N. Y.) **87**, 599 (1971).
40. Mirrors have been manufactured by Layertec company.
41. A.M. De Riva, *et al.*, Rev. Sci. Instrum. **67**, 2680 (1996).
42. P. Brax *et al.*, Phys. Rev. D **76**, 085010 (2007); M. Ahlers *et al.*, Phys. Rev. D **77**, 015018 (2008); H. Gies *et al.*, Phys. Rev. D **77**, 025016 (2008).